An Integrated Image Processing System for Leaf Disease Detection and Diagnosis

[1]Mohammed El-Helly, [2]Ahmed Rafea, and [3]Salwa El-Gammal

[1]Central Lab. For Agricultural Expert System (CLAES), Agriculture Research Center (ACR), Giza, Egypt
helly@mail.claes.sci.eg
[2]Computer Science Department, American University in Cairo (AUC)
Rafea@mail.claes.sci.eg
[3]Computer Science Department, Faculty of Computers &Information, Cairo University
Salwa@mail.claes.sci.eg

Abstract. Leaf spots can be indicative of crop diseases, where leaf batches (spots) are usually examined manually and subjected to expert opinion. In this paper, an integrated image processing system is developed to automate the inspection of these leaf batches and helps identify the disease type. The developed system consists of four stages; the first is the enhancement, which includes HSI transformation, histogram analysis, and intensity adjustment. The second stage is segmentation, which includes adaptation of fuzzy c-mean algorithm parameters to fit the application in concern. Feature extraction is the third stage, which deals with three features, namely; color, size, and shape of the spots. The fourth stage is classification, which comprises back propagation based neural networks. This system has been applied to cucumber crop where the following diseases have been identified, powdery mildew, leaf miner, and downy mildew.

1 Introduction

Vegetable crops suffer from many leaf batches. Leaf batches differ in color, shape and size according to the cause. Leaf batches happen as a result of plant pathogens (fungi, Bacteria, and Virus diseases), insect feeding (sucking insect pests), plant nutrition (lack of micro elements) [1,2,3]. The importance of fungal diseases came from its great distribution, short life cycle, and propagation [1]. In agriculture mass production, it is needed to discover the beginning of plant diseases batches early to be ready for appropriate timing control to reduce the damage, production costs, and increase the income [2,3,5]. Plant leaves are considered the first station for the rest and germination of bacterial, fungal capsules due to the suitable macro environment [3,6]. Leaf batch characteristics play a curial role in differentiating between the different causes. The diagnosis of leaf batches may cause some confusion due to the similarities in batch's shape, size and color but only an expert could identify it. The first step in fighting against these leaf batches is the adequate recognition of their presence that i.e. correct diagnosis. An abnormal symptom is an indication to the presence of the disease, and hence, can be regarded as an aid in diagnosis. Spots are

considered the important units indicating the existence of diseases. In this work an integrated image processing system has been proposed aiming at the identification of these leaf spots. The development of such an intelligent system is justified by its economical relevance and by hard effort necessary to perform a correct diagnosis. This includes the knowledge and experience accumulated by the human expert. Other important aspects are the speed, safety, and reliability of the response of the system.

2 Architecture of the Proposed System

In order to diagnose the cause of the symptom by using an automated tool, so image-processing system has been developed to automate the identification and classification of the leaf batches into specific disorder. As shown in Fig 1, the system consists of three main components: image analyzer, feature repository, and classifier. The processing that was done by using those components is divided into two phases. The first processing phase is the offline phase. In this phase, a large set of defected input images was processed by image analyzer for extracting abnormal features. Then these features were stored in the feature repository for later usage by the classifier. The second processing phase is an online phase, in which the abnormal feature of a specific defected image is extracted by image analyzer and then classified by the classifier into a specific disorder. The image analyzer components are described in Section 3. Section 4 deals with the feature repository. The classifier is discussed in section 5.
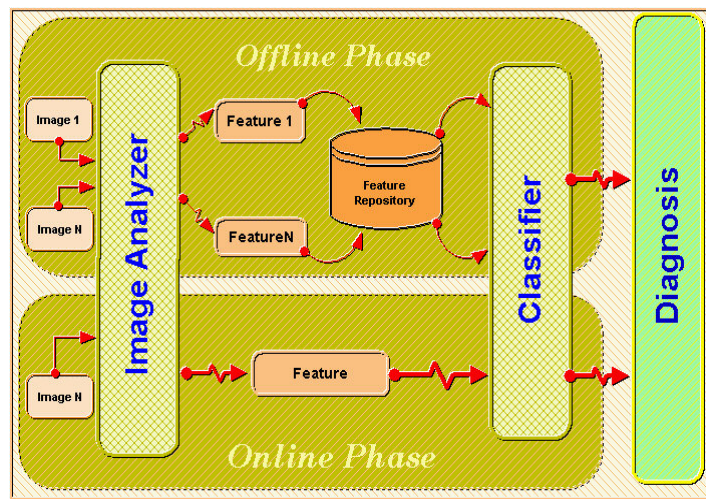

Fig. 1: Overall Structure of the System

3 Image Analyzer

The main purpose of the image analyzer is to extract the abnormal symptom of the defected color image represented in spot size, spot color, and spot shape. As depicted in the Fig. 2 the input of the image analyzer is the acquired defected color image and the output of the image analyzer is the extracted features of the defected image.
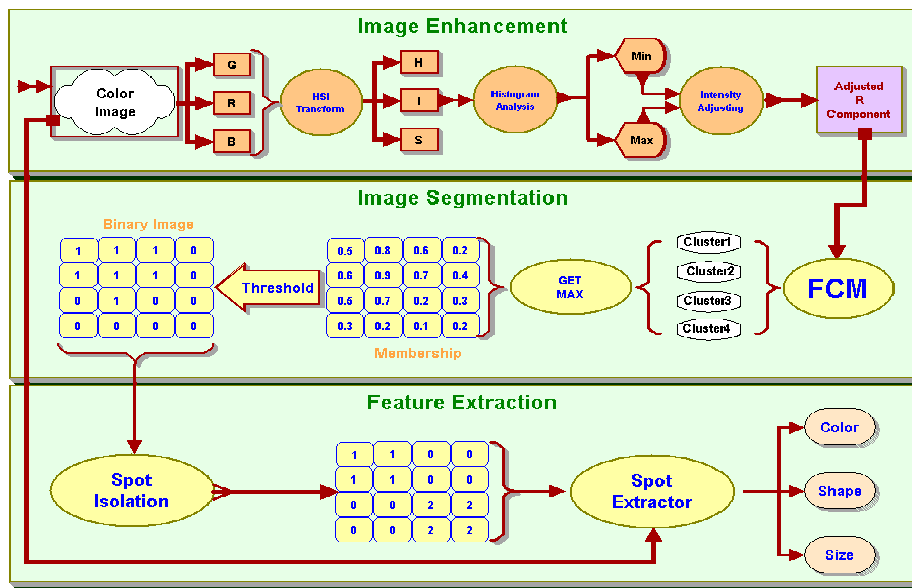

Fig. 2: Image Analyzer Structure

3.1 Image Acquisition

The images are captured by using high resolution 3-CCD color camera (DSC-P1 Cyber-shot, Sony) with 3.3 million-pixel sensitivity, 3X optical zoom lens, auto focus illuminator light, and focal Length 8 - 24mm. The camera was placed at about 60mm from the top of the leaves. The image from the camera is digitized into a 24-bit image with resolution 720 x 540 pixels.

The data set is divided into two groups: The first group was taken in the cucumber green house at Central Lab for Agricultural Expert System (CLAES). This group includes three categories of spotted defected image; those images are for powdery mildew, leafminer, and downy mildew disorders. Fig. 3 represents an example of those defected images. The other part of this group consists of a set of normal images and a set of images used as a negative example in a training phase. The second group is a set of defected leaf images taken from the literature for testing the segmentation phase. These images are related to the following disorders, Gummy stem blight, Scab,

Anthracnose, Pesticide Injury, Phosphorus Def., Whitefly, High temp, and Alternaria Leaf Spot.

Fig. 3: Sample of defected image

3.2 Enhancement Phase

Image Enhancement is a sub-field of image processing and consists of techniques to improve the appearance of an image, to highlight important features of an image, and to make this image more suitable for use in a particular application (e.g., make certain features easier to see by modifying the colors or intensities).

The abnormality of the defected leaves is revealed by the apperance of the spots. From the inspection of the infected leaves it was found that the spots have intensity values higher than other normal tissues. To extract those abnormal tissues, so our enhancement processing for the infected leaves as debicted in Fig. 2 consists of three steps. The first step is the transformation of the defected image into HSI color space. The second step is analyzing the histogram of the intensity channel to get the threshold by which we can increase the contrast of the image. The final step is to adjust the intensity of the image by applying the thresholds.

HSI Transformation. Color is perceived by humans as a combination of R, G, B bands, which are called primary colors. Several color spaces, such as HSI and CIE are derived from primary colors using either linear or nonlinear transformations, and utilized in color image segmentation

HSI (hue-saturation-intensity) system is a commonly used color space in an image processing, which is more intuitive to human vision [7-10]. HSI system separates color information of an image from its intensity information. Color information is represented by hue and saturation values. While intensity describes the brightness of an image[11]. The HSI color system has a good capability of representing the colors for human perception, because human vision system can distinguish different hues easily. Whereas, the perception of different intensity or saturation does not imply the recognition of different colors[11]. The formula of HSI is:

$$H = ArcTan\left(\frac{\sqrt{3}(G-B)}{(R-G)+(R-B)}\right) \qquad \textbf{(1)}$$

$$I = \frac{(R + G + B)}{3} \qquad (2)$$

$$S = 1 - \frac{Min(R, G, B)}{I} \qquad (3)$$

The results of the HSI transformation are shown in the Figure 4
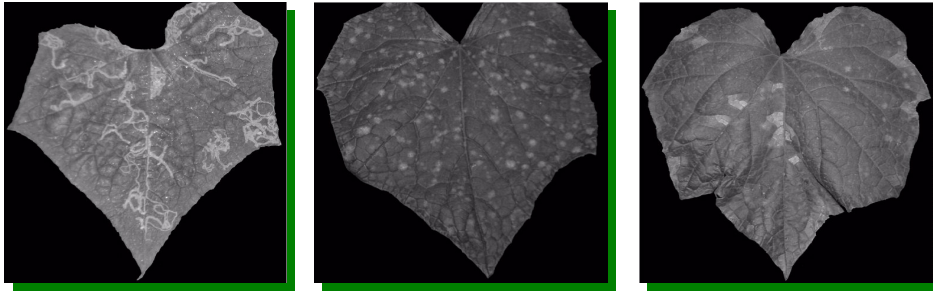
Fig. 4: Images after HSI transformation

Histogram Processing. The histogram of a digital image with gray levels in the range [0-L-1] is a discrete function $p(r_k)$

$$p(r_k) = \frac{n_k}{n} \quad k = 0,1,....,L-1 \qquad (4)$$

Where L is the number of gray levels usually 256, n the total number of the image pixels, n_k is the number of pixels having intensity level k. The image histogram carries important information about the image content. Loosely speaking, $p(r_k)$ gives an estimate of the probability of occurrence of gray level r_k. A plot of this function for
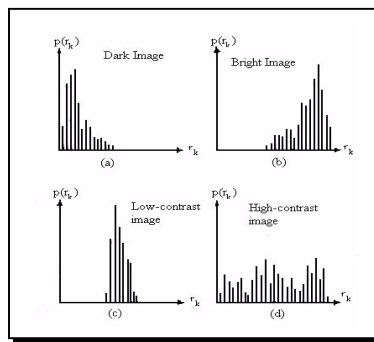

Fig. 5: Histograms corresponding the four basic image types

all values of k provides a global description of the appearance of an image. If the pixel values are concentrated in the low image intensities as can be seen in Fig. 5(a), the image is 'Dark'. A 'Bright' image has a histogram that is concentrated in the high image intensities, as seen in Fig. 5(b), .In Fig. 5(c), the histogram has a narrow shape, which indicates little dynamic range, and thus corresponds to an image having low contrast. As all gray levels occur toward the middle of the gray scale, the image would appear a murky gray. In *Fig. 5(d)*, the histogram possesses significant spread, corresponding to an image with high contrast. The histogram does give us useful information about the possibility for contrast enhancement. The results of generating the histogram of the defected image are shown in Figure 6
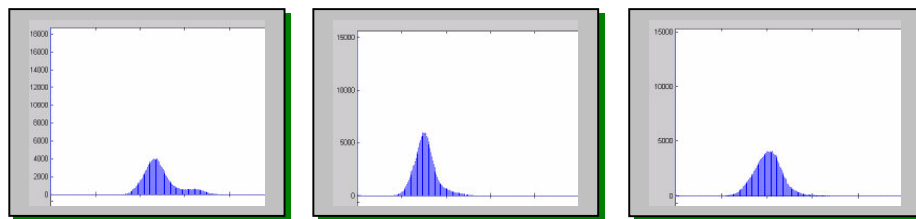
Fig. 6: Histogram of the Defected Image of Figure 4

Intensity Adjustment. Frequently, image intensity values do not make full use of the available dynamic range. This can be easily observed in the histogram shown in Fig. 7. Intensity adjustment is a technique for mapping an image intensity values to a new range. This situation can be corrected by stretching the histogram over the available dynamic rang as shown Fig. 8. We generally map the minimum value to zero and the maximum value to 1.
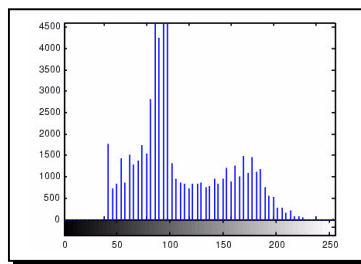
Fig.7: Low Contrast Image
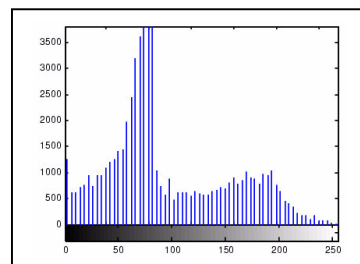
Fig.8: High Contrast Image

The appropriate transformation is given by the following formula

$$
b[m,n] = \begin{cases} 0 & a[m,n] \le p_{low} \\ \left(\dfrac{a[m,n] - p_{low}}{p_{high} - p_{low}} \right)^{\gamma} & p_{low} < a[m,n] < p_{high} \quad \textbf{(5)} \\ 1 & a[m,n] \ge p_{high} \end{cases}
$$

Depending on the value of Gamma (γ), the mapping between values in the input and output images may be linear or nonlinear. Gamma can be any value between 0 and infinity. If gamma is 1, the mapping is linear. If gamma is less than 1, the mapping is weighted toward higher (brighter) output values. If gamma is greater than 1, the mapping is weighted toward lower (darker) output values.
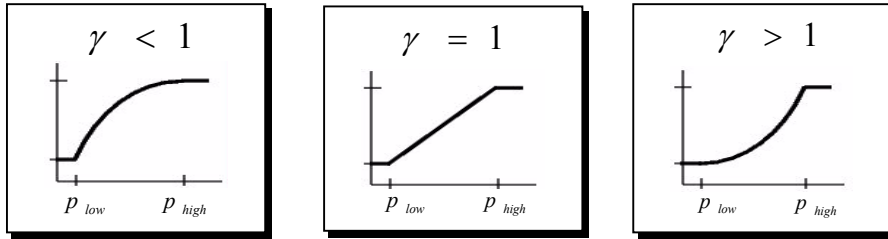
Fig. 9: Gamma Correction

To get the p_{low} and p_{high} of the histogram we have to calculate the probability density function of the histogram as shown in the Fig. 10
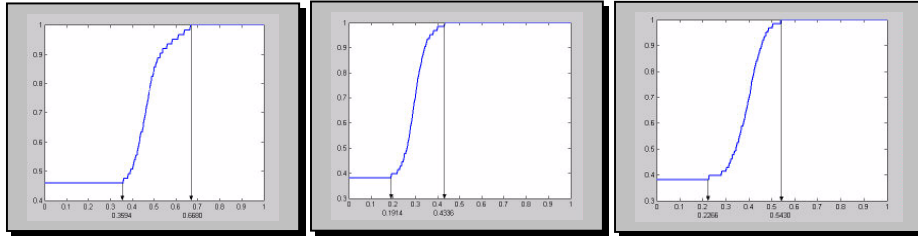
Fig. 10: PDF for histogram of Figure 6

After getting the two thresholds p_{low} and p_{high} for the images, we have applied those thresholds to the intensity component as described in eq. 5. We have choosed 2 for gamma to move toward the darker side. The results are shown in Fig. 11
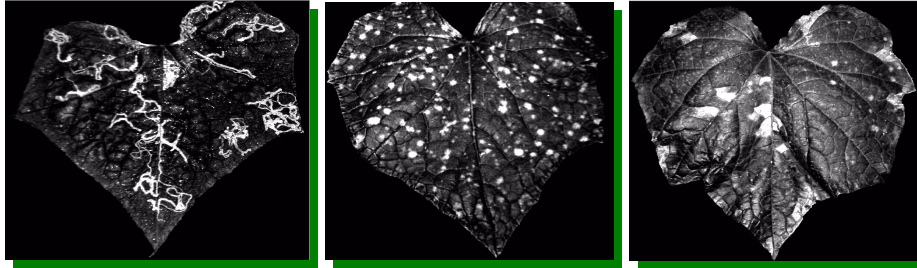
Fig. 11: Images after Intensity adjustment

3.2 Segmentation Phase

Image segmentation is the first step in image analysis and pattern recognition. It is a critical and essential step and is one of the most difficult tasks in image processing, as it determines the quality of the final result of analysis. The problem of segmentation has been broadly investigated by scientists using both classical [12,13] and fuzzy based techniques [14-17]. Classical segmentation approaches take crisp decisions about the regions. However, regions in an image are not always crisply defined and uncertainty can arise within each level of image processing, as in our addresses. Most plant images are represented by overlapping gray-scale intensities for different tissues . . In addition, borders between tissues are not clearly defined and memberships in the boundary regions are intrinsically fuzzy. Fuzzy set theory provides a mechanism to represent and manipulate the uncertainty and the ambiguity. Therefore fuzzy clustering turns out to be particularly suitable for the segmentation of plant images. One widely used algorithm is the fuzzy c-means (FCM) algorithm, which was first presented by Dunn [18], further developed by Bezdek [19]. Subsequently, it is revised by Rouben[20], Gu [21], and Xie [22]. However, Bezdek's FCM remains the most commonly used algorithm.

The segmentation of defected plant images involves partitioning the image space into different cluster regions with similar intensity image values. The success of applying FCM to fit the segmentation problem depends mainly on adapting the input parameter values [23,24]. As a consequence, if any of the parameter is assigned an improper value, the clustering results in a partitioning scheme, that is not optimal for the specific data set and that leads to a wrong decision. These parameters include, the feature of the data set, the optimal number of clusters, and the degree of fuzziness. Based on experiments with these parameters, we've shown that a good cluster number for leaf spots is 4, and the degree of fuzziness is 2 [25]. We've applied those parameters to our data set and the results are presented in Figure 12-15. In this Figures, the top row represents the original defected input images, while the bottom row represents abnormalities detected via segmentation.
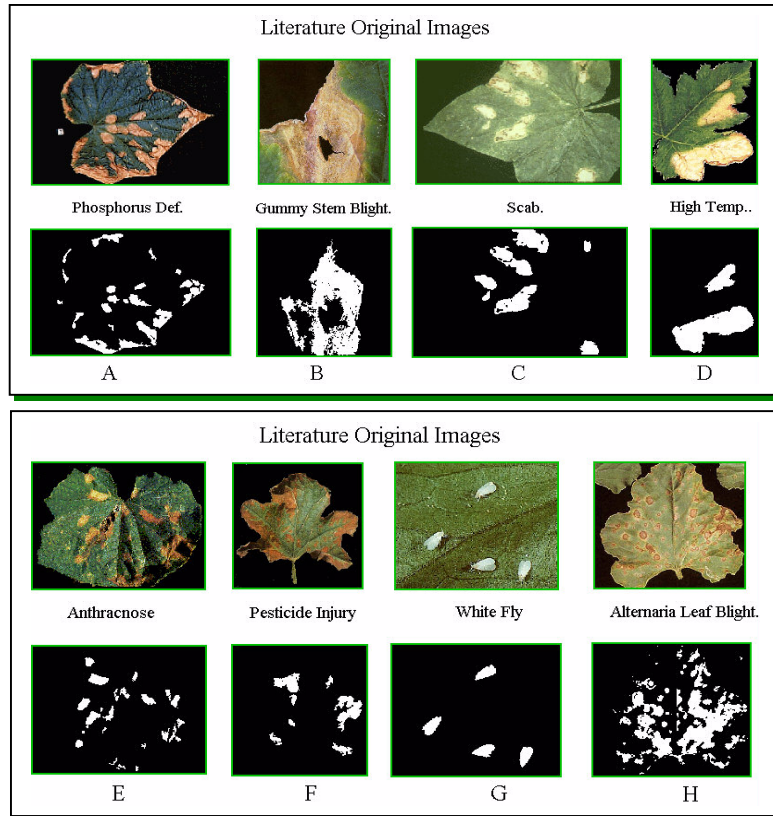
Fig. 12: Segmentation Results on some Literature Images
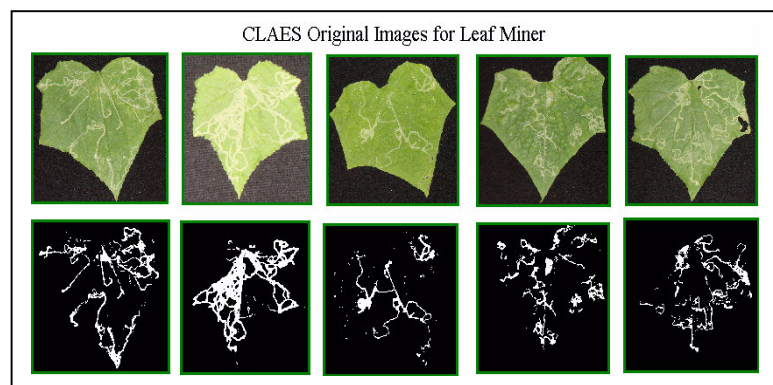
Fig. 13: Original and segmented CLAES images for Leafminer
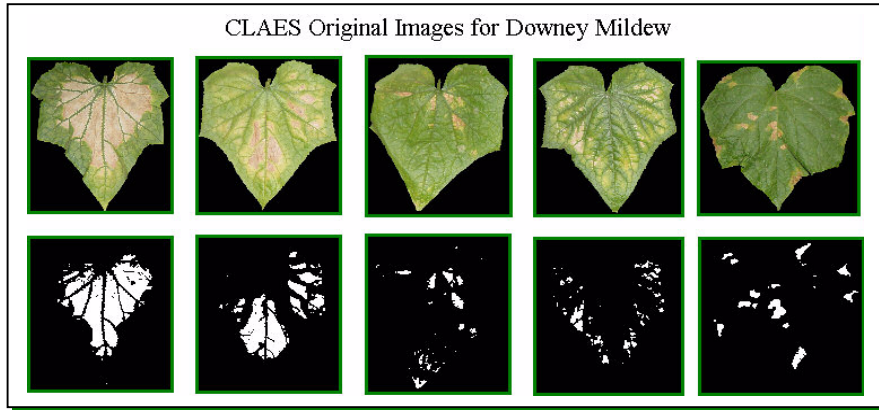
Fig. 14: Original and segmented CLAES images for Downey
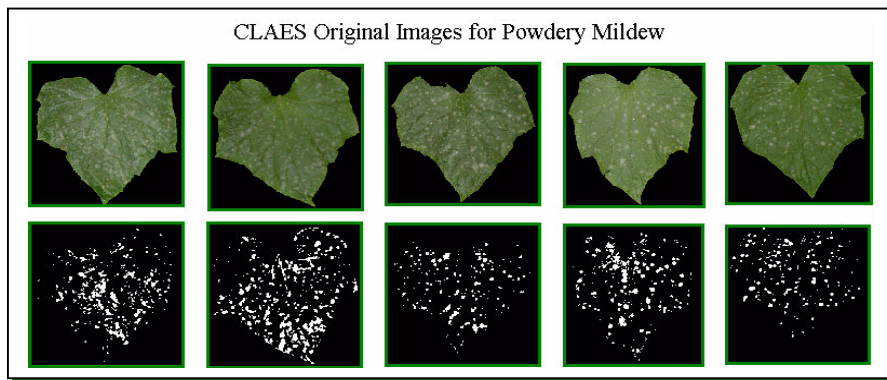
Fig. 15: Original and Segmented CLAES Images for Powdery

3.3 Feature Extraction phase

The third phase is the feature extraction phase. The purpose of the feature extraction is to reduce the image data by measuring certain features or properties of each segmented regions such as: color, shape, or texture. This phase consists of two steps, mainly spot isolation, and spot extraction.

Spot Isolation. Often, a segmented image consists of a number of spots. In order to extract features from the individual spot, it is necessary to have an algorithm that identifies each spot. To identify the spots, we label each spot with a unique integer and the largest integer label gives the number of spots in the image. Such identification algorithm is called component labeling [26]. The following Figure

depicts the binary-segmented image and the labeled image after applying the component-labeling algorithm.

Fig. 16: Labeling Segmented Image

Feature Extraction. In order to recognize the spot category, we measure several numbers of features from the segmented image, to be later used for classification purposes. These features correspond to color characteristics of the spots such as: the mean of the gray level of the red, green, and blue channel of the spots. Other features correspond to morphological characteristics of the spots [26,27] such as:

1. The length of the principal axes, Major and Minor axes length of a spot.
2. The diameter of a spot, is measured as:

$$SQRT(4*Area/PI) \tag{6}$$

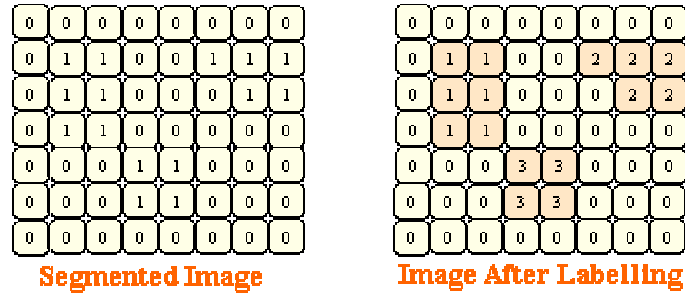3. Eccentricity Measure: also called circularity ratio, its value between 0, 1, the spot whose circularity ratio is zero is actually a circle, while the spot whose circularity ratio is one is actually line. The circularity ratio is computed as :

$$2*SQRT((Major/2)\char`\^2-(Minor/2)\char`\^2)/Major) \tag{7}$$

4. Compactness Measure: also called solidity ratio, has a value between 0,1. If the spot has a solidity value equal to 1, this means that it is fully compacted. It is the ratio between the spot border length (Convex Area) and the area of the spot. The formula is computed as:

$$SpotArea/ConvexArea \tag{8}$$

5. Extent Measure: also called rectangularity ratio, has a value between (0 1], when this ratio has the value one, then the shape is perfectly rectangle, is computed as:

$$SpotArea/BoundingBoxArea \tag{9}$$

6. Euler's Number Measure: This measure describes a simple, topologically invariant property of the spot. It is computed as the number of objects in the region minus the number of holes in those objects.
7. Orientation Measure: is the angle in degrees between the x-axis and the major axis length of the spots.

Figure 7 presents calculated measures for the three previous classes of spots.

Class Name	Segmented Image	Major Axes	Minor Axes	Diameter	Eccentricity Circularity	Compactness Solidity	Extent Rectangularity	Euler's Number	Orientation
Downy		25	17	19	0.7	0.8	0.6	1	96
Powdery		15	13	13	0.4	0.9	0.7	1	27
Leafminer		57	16	16	0.95	0.33	0.2	1	-16

Fig. 17: Morphological measurements of the three classes

4. Features Database

The features database is the component used to store the outputs of the feature extraction phase for later usage by the classifier. The database is a relational one, which consists of two tables namely a disorder table, which is used to keep track of disorders that have been processed and a feature table, which is used to store the spot features for each disorder. The database created contains 1500 records 300 records per each class.

5 The Classifier

Before the on-line processing is done, the system needs to be manually trained using a set of training samples. An Artificial Neural Network ANN was used to perform our classification task. There are many different types of ANNs. The most widely used is the Back Propagation ANN. This type of ANN is excellent for performing classification task [28,29]. The developer of ANN has to answer the main question: which configuration of the ANN is appropriate for a good out-of-sample prediction? The configuration of ANN needs to be determined accurately to give an optimal classification result. This configuration includes the number of layers, the number of neurons for each layer, and the minimal number of training samples. This configuration is also called the topology of the ANN. It is known that too many neurons degrade the effectiveness of the model, leads to the undesirable consequences, long training times, and local minima. Large number of connection weights in the ANN model may cause over-fitting and loss of the generalization capacity. On the other hand, choosing too few neurons may not capture the full complexity of the data. Many heuristic rules were suggested for finding the optimal number of neurons in the hidden layer, and several techniques were now available. Most of them employ trial-and-error methods, in which the ANN training starts with a small number of neurons, and additional neurons are gradually added until some performance goal is satisfied [30]. Unfortunately, there is no theoretical consideration for determining the optimal network topology for the specific problem. We used a well known statistical analysis technique called ANOVA, for determining the optimal

configuration of the neural network. A good introduction to the analysis of variance (ANOVA) is given by [31].

5.1 Experimental Procedure

The experiment was considered to determine the best structure of the neural network that gives the best identification percentage of the following classes: class A (Downy), class B (leafminer), class C (powdery), class D (Normal), and class N (Negative). Also, the experiment is designed to investigate the influence of each factor on the identification percentage. Those factors are a number of learning samples, number of neurons, and a number of hidden layers (Table 1).

Table 1: Experiment Design for Neural Network Factors

Example	Neurons	Layers	A	B	C	D	N
50-250	5	One	0.44	0.26	0.52	0.52	0.23
		Two	0.68	0.7	0.68	0.55	0.43
	10	One	0.55	0.67	0.6	0.43	0.22
		Two	0.86	0.4	0.52	0.48	0.3
	15	One	0.6	0.43	0.39	0.53	0.27
		Two	0.38	0.59	0.53	0.62	0.25
	20	One	0.43	0.3	0.5	0.44	0.32
		Two	0.46	0.48	0.42	0.57	0.23
100-200	5	One	0.44	0.26	0.4	0.54	0.31
		Two	0.62	0.77	0.69	0.68	0.41
	10	One	0.9	0.37	0.81	0.87	0.28
		Two	0.79	0.51	0.79	0.77	0.24
	15	One	0.83	0.47	0.52	0.55	0.36
		Two	0.73	0.44	0.52	0.43	0.44
	20	One	0.56	0.55	0.54	0.35	0.31
		Two	0.53	0.66	0.64	0.48	0.38
150-150	5	One	0.81	0.75	0.63	0.92	0.32
		Two	0.83	0.59	0.82	0.77	0.31
	10	One	0.76	0.52	0.75	0.46	0.27
		Two	0.79	0.72	0.62	0.52	0.61
	15	One	0.72	0.69	0.56	0.53	0.37
		Two	0.8	0.63	0.67	0.33	0.6
	20	One	0.52	0.33	0.54	0.58	0.46
		Two	0.67	0.61	0.77	0.69	0.55
200-100	5	One	0.79	0.5	0.87	0.57	0.22
		Two	0.78	0.64	0.78	0.93	0.89
	10	One	0.71	0.52	0.7	0.83	0.6
		Two	0.77	0.73	0.76	0.6	0.5
	15	One	0.66	0.49	0.63	0.48	0.41
		Two	0.77	0.76	0.77	0.69	0.6
	20	One	0.62	0.39	0.8	0.67	0.43
		Two	0.63	0.72	0.7	0.68	0.48
250-50	5	One	0.5	0.56	0.78	0.68	0.02
		Two	0.86	0.74	0.94	0.98	0.92
	10	One	0.54	0.56	0.82	0.84	0.7
		Two	0.66	0.72	0.84	0.8	0.56
	15	One	0.5	0.52	0.86	0.82	0.52
		Two	0.62	0.74	0.84	0.9	0.78
	20	One	0.34	0.56	0.5	0.88	0.68
		Two	0.6	0.66	0.8	0.76	0.72

Learning Samples. Different combinations of learning samples categories were used to investigate the influence of increasing the number of learning samples on the classifier accuracy. Those categories are: train with 50 sample and test with 250 sample, train with 100 sample and test with 200 sample, train with 150 sample and test with 150 sample, train with 200 sample and test with 100 sample, and finally train with 250 sample and test with 50 sample.

Neurons. Different number of neurons was used to investigate the increasing number of neurons on the classifier accuracy. Those numbers are 5,10,15, and 20.

Layers. The last factor is the number of hidden layers. The tried number is one hidden layer and two hidden layers, which are used to determine how many layers are necessary to give the highest accuracy of the classifier.

5.2 Experimental Analysis

After designing the experiments as depicted in Table1, the ANOVA table is constructed to measure the significance of each factor. The results is shown in Table 2

Table2: ANOVA Table for Main Effects

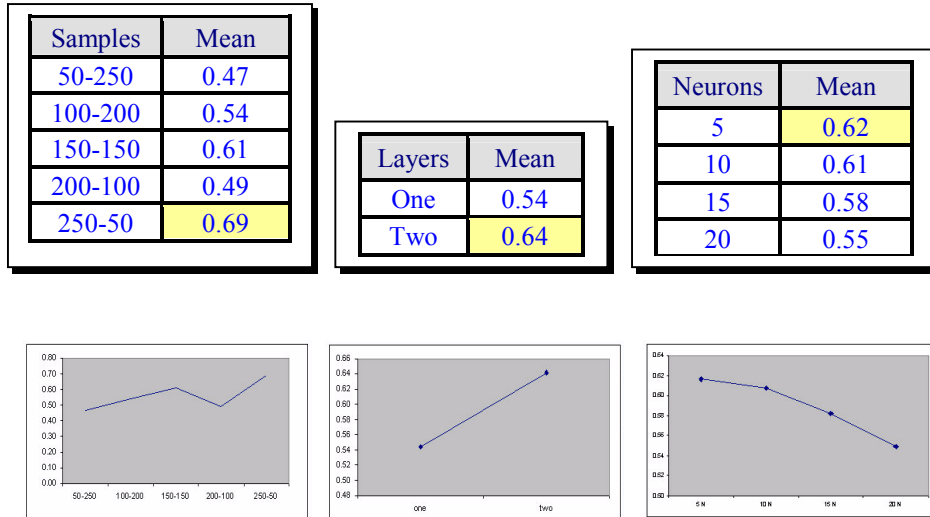| Main Effects	SS	DF	MS	F	Significance
Layers	0.47	1	0.47	18.5	Highly
Neurons	0.17	3	0.055	2.22	Not
Samples	1.24	4	0.31	12.07	Highly

Where SS is the sum of square, DF is the degree of freedom, MS is the mean of square, and F is the ratio of the variance between groups and variance within groups. Examining the results in Table3, it is seen that:

- The layers factor has a high significance on the identification percentage. This means that using two layers has a better effect on the identification percentage than one layer.
- The samples factor has a high significance on the identification percentage. This means that using 250 training samples has a better effect on the identification percentage than using 50 samples.
- The neurons factor is not significant on the accuracy of the classifier. This means that using five neurons are sufficient.

The mean of each factor regardless the other factors were calculated to measure the effects of each factor individually on the classifier accuracy. These results are depicted in table 3 and plotted in Fig.18.

Table 3: Mean of each factor, Sample, Layer, and Neurons

Samples	Mean
50-250	0.47
100-200	0.54
150-150	0.61
200-100	0.49
250-50	0.69

Layers	Mean
One	0.54
Two	0.64

Neurons	Mean
5	0.62
10	0.61
15	0.58
20	0.55

Fig 18: Mean of each factor, Sample, Layer, and Neurons

It is obvious of Fig. 18 that using small number of neurons, large number of layers, and large number of training samples lead to a much better ratio of identification. So, the optimal decisions for designing the classifier 11-5-5-1, and training this classifier with 250 samples. This results is depicted in Table 4.

Table 4: Optimal choice for classifier

Examples	Neurons	Layers	A	B	C	D	N
250-50	5	Two	0.86	0.74	0.94	0.98	0.92

As shown in Table 4, the capability of the classifier to identify normal leaves is 98%, which is the highest recognition percentage. This can be attributed to the fact that normal leaves exhibit no abnormal features, which makes it easy for the classifier to identify them. The third highest recognition percentage was for unknown diseases. This high recognition percentage is due to the fact that the classifier has been trained extensively to recognize 3 specific diseases. As a result, the classifier is capable of identifying the features that best point to them, as well as, features that do not indicate their presence. The second highest identification percentage was for the powdery

mildew disease. This can be explained by the ease by which features related to that disease can be detected. The fourth, and fifth percentages were for downy mildew and leafminer diseases. These percentages are acceptable for those diseases because there was an overlap in the appearance of some symptoms related to those disorders.

6 Conclusions

In this paper we have developed an integrated image processing system capable of diagnosing three disorders, Downy mildew with percentage 84%, Leafminer with percentage 74%, and Powdery mildew with percentage 94%. Also, the system is capable of deciding the normal leaves with a percentage 98%. Moreover, the system is capable to recognizing the unknown disorder with a percentage 92%.

A set of features was selected to be extracted using feature extraction phase, and those features were stored in the feature database, which is designed for this purpose.

We have used feed-forward neural networks with two hidden layers and the standard back propagation rule as the training algorithm. Each neural network node uses a sigmoid transfer function and the objective function to be minimized was the MSE.

A statistical experiment was designed for different ANN configurations, and analyzed using ANOVA approach for selecting the optimum structure of neural network that gives good identification results. The decision of the topology of ANN to give a high identification percentage was two hidden, five neurons per each layers, and 250 for number of training samples.

Reference

[1] Agrios, G.N. 1997. Plant Pathology, 4th Edition. Academic Press.
[2] Barnett, H.L. and Hunter, B.B. 1998. Illustrated Genera of Imperfect Fungi, 4th Edition. APS Press.
[3] Berger, R. D. and Jones, J. W., 1985. A general model for disease progress with functions for variables latency and lesion expansion on growing host plant. Phytopathology. 75: 792-797.
[4] Campbell, C. L., and Madden, L. V., 1990. Introduction to Plant Disease Epidemiology. John Wiely & Sons, New York City. 532 pp.
[5] Shurtleff, M.C. and Averre, A.W. 1997. The Plant Diseases Clinic and Field Diagnosis of Abiotic Diseases. APS Press.
[6] Simone, G.W., Pohronezny, K.L. and Blake, J.H. 1988. Training in Microscope Diagnosis of Plant Diseases. July 26-27.
[7] T. L. Huntsberger, C. L. Jacobs and R. L. Cannon, 1985. Iterative Fuzzy Image Segmentation, Pattern Recognition, Vol. 18, No. 2, 131-138.
[8] T. Carron and P. Lambert, 1994. Color Edge Detector Using Jointly Hue, Saturation and Intensity", IEEE International Conference on Image Processing, Austin, USA, 977-081.

[9] Y. Rui, A. C. She and T. S. Huang, 1996. Automated Region Segmentation Using Attraction-based Grouping in Spatial-color-texture space, International Conference on Image Processing, A, 53-56.

[10] W. S. Kim and R. H. Park, 1996. Color Image Palette Construction Based on the HSI Color System for Minimizing the Reconstruction Error, IEEE International Conference on Image Processing, C, 1041-1044.

[11] H. D. Cheng, X. H. Jiang, Y. Sun and Jing Li Wang, 2001. Color Image Segmentation: Advances & Prospects, Pattern Recognition, Vol.34, PP.2259-2281.

[12] Gonzaliz RC., Woods RE. 2002. Digital image processing, Pearson Education. Inc.

[13] L. Spirkovska. 1993. A Summary of Image Segmentation Techniques, NASA Technical Memorandum 104022, June.

[14] Bezdek J.C., R. Ehrlich, W. Full., 1984. FCM: The Fuzzy c-mean Clustering Algorithm, Computers and Geoscience, 10, pp.191-203.

[15] Chi Z., Yan H., Pahm T., 1996. Fuzzy Algorithms: With Applications to Image Processing and Pattern Recognition, World Scientific.

[16] Dzung L., Chenyang X., Jerry L., 2001. A Survey of Current Methods In Medical Image Segmentation, Technical Report JHU/ECE 99-01, The Johns Hopkins University.

[17] S. K. Pal., 1992. Image Segmentation Using Fuzzy Correlation, Information Sciences, 62, 223-250.

[18] Dunn, J. C. 1974. Well-separated clusters and the optimal fuzzy partitions, Journal of Cybernetics, 4: 95-104.

[19] Bezdek, J. C. 1981. Pattern Recognition with Fuzzy Objective Function Algorithms, Plenum Press, NewYork, NY.

[20] Rouben, M., 1982. Fuzzy clustering algorithms and their clustering validity, European Journal of Operational Research, 10: 294-301.

[21] Gu. T., Dubuission B., 1990. Similarity of classes and fuzzy clustering, Fuzzy Sets and Systems, 34: 213-221.

[22] X. L. Xie, G. Beni., 1991. A Validity Measure for Fuzzy Clustering, IEEE Trans. on Pattern Analysis and Machine Intelligence, Vol. 13, No. 8, 841-847.

[23] M. Halkidi, Y. B., M. V., 2002. Cluster Validity Methods: Part I, SIGMOD Record, June.

[24] M. Halkidi, Y. B., M. V., 2002. Cluster Validity Methods: Part II, SIGMOD Record, September.

[25] El-Helly M., Onsi H., Rafea A., El-Gamal S., 2003. Segmentation Technique for Detecting Leaf Spots in Cucumber Crop Using Fuzzy Clustering Algorithm. 11th International Conference on AI (ICAIA).

[26] Sonka M., Hlavac V., BoyLE R., 1999. Image Processing Analysis and Machine Vision, Brooks/Cole Publishing Company, USA.

[27] Matlab Doc. 2002. Image Processing Toolbox User's Guide Version 3. Mathworks Incorporation.

[28] Hecht-Nielsen, R., 1990. Neurocomputing. Addison Wesley.

[29] Hertz, J., Krogh, A., and Palmer, R., (1991). Introduction to the Theory of Neural Computation. Addison-Wesley: Redwood City, California.

[30] Boger Z. Weber R. 2000. Finding an Optimal Artificial Neural Network Topology in Real-Life Modeling. In: Proceedings of the ICSC Symposium on Neural Computation, Article No. 1403/109.

[31] Norman R., 1983. Introduction to social statistics, McGraw-Hill Inc.